Macromolecules
ARTICLE

*Macromolecules* **2010**, *43*, 5405–5410 **5405**
DOI: 10.1021/ma1006057

# Transition of Large Compound Micelles into Cylinders in Dilute Solution: Kinetic Study

**Weiran Lin, Cui Zheng, Xinhua Wan,* Dehai Liang,* and Qifeng Zhou**

*Beijing National Laboratory for Molecular Sciences, Key Laboratory of Polymer Chemistry & Physics of Ministry of Education, College of Chemistry & Molecular Engineering, Peking University, Beijing 100871, P. R. China*

*Received March 19, 2010; Revised Manuscript Received May 14, 2010*

ABSTRACT: Time-resolved laser light scattering, combined with transmission electron microscopy, was employed to study the kinetics of the sphere-to-rod transition. The brush−rod block copolymer based on poly[poly(ethylene glycol) monomethyl ether methacrylate] and poly{(+)-2,5-bis[4′-((*S*)-2-methylbutoxy)-phenyl]styrene}, $PEGMA_{37}$-*b*-$MBPS_{141}$, formed spherical large compound micelles (LCM) in mixed solvent of THF and water. LCM underwent the transition to large compound rod (LCR) in the time scale of hours, and the transition was favored at higher polymer concentration and at intermediate water content. It was also found that a large amount of free polymer chains existed throughout the transition process. The depletion force generated by the free polymer chains was estimated to be in the order of $0.1kT$. Therefore, besides the instability or defects of the LCM, the depletion effect also made a positive contribution to the sphere-to-rod transition.

## Introduction

In the past few decades, many attempts have been made to gain an insight into the assembly of amphiphilic block copolymers in solution, which may help to understand the organization mechanism of cellular tissues.[1−10] The nanostructures assembled by block copolymers were determined by a number of factors, such as chemical nature of each block and block ratio. These factors built a delicate balance of the overall surface tension with chain stretching inside and outside the assembled structure.[11,12] Through a proper control over the balance, various morphologies could be obtained in solution. Besides the three basic structures—spheres, cylinders, and bilayers[13,14]—the complex or combined morphologies, e.g., hollow tubes, branched short rods, and interconnected bicontinuous rods, were observed under certain conditions.[15] In addition, the flexibility of the block, e.g. rigid rod versus flexible coil, also showed a profound effect on the assembly of the block copolymers. Rod−coil block copolymers, consisting of both flexible and rigid segments, had the capacity to form desirable morphologies and thus attracted a great deal of attention from biologists, chemists, and physicists.[8,16−23]

As various morphologies were observed, the transition of different morphologies became an active research area.[24−28] The most widely studied case was the sphere-to-rod transition of micelles.[29−42] One of the typical polymer samples was the triblock copolymer of poly(ethylene oxide)−poly(propylene oxide)−poly(ethylene oxide) (EO−PO−EO), whose sphere-to-rod transition in dilute solution was induced by a jump in temperature. Both laser light scattering (LLS)[29,30] and small-angle neutron scattering (SANS)[31] have been applied to determine the changes in morphology. Using polystyrene-*b*-poly(acrylic acid) in mixed solvents of dioxane and water, Eisenberg and co-workers investigated the kinetics of sphere-to-rod and rod-to-sphere transitions by turbidity measurement and transmission electron microscopy (TEM).[32] They proposed a two-step mechanism for sphere-to-rod transition: formation of irregular "pearl necklace" via spherical collision, followed by reorganization into smooth cylindrical rods, whereas the reverse transition began with bulb formation from ends of the cylinders, followed by the release of bulbs to form spheres. However, Ma et al.[33] suggested that the decomposition of the cylinders did not merely begin from the ends but experienced many morphological intermediates during the rod-to-sphere transition. Recently, Denkova et al.[34] studied the sphere-to-rod transition of $EO_{20}PO_{70}EO_{20}$ induced by adding inorganic salt and ethanol. It was suggested that the growth of micelle was controlled mainly by random coagulation/fragmentation reactions. The unimer was also detected by dynamic light scattering during the growth stage. Shen et al.[35] investigated the sphere-to-cylinder transition by using poly(ferrocenyldimethylsilane-*b*-2-vinylpyridine) (PFS−P2VP) in methanol, a selective solvent for P2VP. The block copolymer formed stiff, uniform fiber-like micelles with cores of 10 nm and lengths between 20 and 50 $\mu$m. They attributed the driving force to the crystallization of PFS block.

Online monitoring the kinetics of sphere-to-rod transition is a practical approach to reveal the transition mechanism. Laser light scattering is a powerful technique to discover the details, provided that the transition is in the order of minutes or slower.[43] In 1996, Eisenberg and co-workers observed large compound rod (LCR) with a diameter of ~550 nm from 3.0 wt % $PS_{210}$-*b*-$PEO_{45}$ in DMF.[15] Besides the rod, a large amount of solid spheres with diameters less than 70 nm was also observed in TEM image. Our previous study on the brush−rod diblock copolymer with poly[poly(ethylene glycol) monomethyl ether methacrylate] as the hydrophilic segment and poly{(+)-2,5-bis[4′-((*S*)-2-methylbutoxy)-phenyl]styrene} as the hydrophobic segment, $PEGMA_{37}$-*b*-$MBPS_{141}$, also evidenced the coexistence of solid spheres and LCRs by TEM.[44] Since the diameter of the LCR was much larger than the length of the fully stretched polymer chains, the LCR must be constructed by the aggregation of some primary structures via possibly the sphere-to-rod transition. The LCR was much larger in size and volume than regular rod; the formation and transition

*Corresponding authors: e-mail dliang@pku.edu.cn, Tel 10-86-62756170 (D.L.); e-mail xhwan@pku.edu.cn, Tel 10-86-62754187 (X.W.).



Published on Web 05/21/2010

**Scheme 1. Chemical Structure of the Brush−Rod Diblock Copolymer $PEGMA_{37}$-*b*-$MBPS_{141}$**

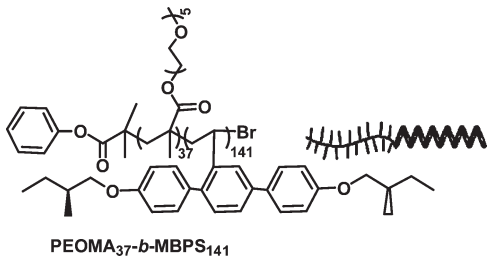


process could be slow in kinetics, which allowed us to monitor the process in detail by time-resolved laser light scattering. In this work, we studied the $PEGMA_{37}$-*b*-$MBPS_{141}$ in THF at 1.0 mg/mL by dynamic light scattering, static light scattering, and TEM. The aggregation of $PEGMA_{37}$-*b*-$MBPS_{141}$ was initiated by the addition of water, which was a selective solvent for PEGMA block. LCR was formed at certain water content. Another reason for choosing $PEGMA_{37}$-*b*-$MBPS_{141}$ was that the single polymer chain was detected easily by LLS, and we can determine the role of single polymer chains during the sphere-to-rod transition.

## Experimental Section

**Laser Light Scattering (LLS).** The brush−rod block copolymers, $PEGMA_{37}$-*b*-$MBPS_{141}$ (Scheme 1), were synthesized and purified according to a known procedure.[44] The polymer samples with known amount were dissolved in THF (HPLC grade) at least one night before the measurement to obtain homogeneous solutions. For the laser light scattering measurement, about 2 mL polymer solution was filtered directly into a dust-free cylindrical light-scattering cell through a 0.22 $\mu$m pore size Millex filter unit (Millipore, Billerica, MA). Deionized water (Milli-Q, 18.2 MΩ) filtered through a 0.22 $\mu$m pore size filter unit was added to the copolymer solution. During the study on the effect of water content, one drop of water (~2.0 wt % of the solution) was added at each interval, and the polymer solution was vortexed at 600 rpm for about 2 min. The sample solution then sat at 25 °C for about 0.5 h before carrying out the measurement. During the study on kinetics, a known amount of water was added in polymer solution in one batch. The time point right after the 2 min vortex at 600 rpm was set as $t_0$.

A commercial laser light scattering spectrometer (Brookhaven Inc., Holtsville, NY) equipped with a BI-200SM goniometer and a BI-TurboCorr digital correlator was used to perform both static light scattering (SLS) and dynamic light scattering (DLS) over scattering angles ranging from 20° to 120°. A 100 mW, vertically polarized solid state laser (GNI, Changchun, China) operating at 532 nm was employed as the light source. In SLS, the angular dependence of the excess absolute time-averaged scattering intensity, also known as the Rayleigh ratio $R_{vv}(\theta)$, was measured. From the angular dependence of $R_{vv}(\theta)$ in a single concentration, the apparent *z*-average root-mean-square radius of gyration $R_{g,app}$ was obtained. In dynamic LLS, the intensity−intensity time correlation function $G^{(2)}(t)$ in the self-beating mode was measured. It is related to the normalized first-order electric field time correlation function $g^{(1)}(t)$. A Laplace inversion program, CONTIN, was applied to analyze $g^{(1)}(t)$ to obtain the hydrodynamic radius, $R_{h,app}$, as well as its distribution. The $R_{g,app}/R_{h,app}$ values were calculated by a combination of the results from SLS and DLS.[45,46]

**Transmission Electron Microscopy (TEM).** Right after LLS measurements, the resulted solution at each stage was poured into a large amount of water to instantly freeze the aggregate structure.[5,6,12] A drop of the sample solution was mixed with a drop of 2% (w/v) aqueous solution of uranyl acetate. The mixture was deposited onto a carbon-coated copper EM grid for a few minutes. Excess solution was blotted away with a strip of filter paper, and the sample grid was dried in air. The morphologies of the aggregates were observed on a JEM-200CX TEM operating at an acceleration voltage of 120 kV.

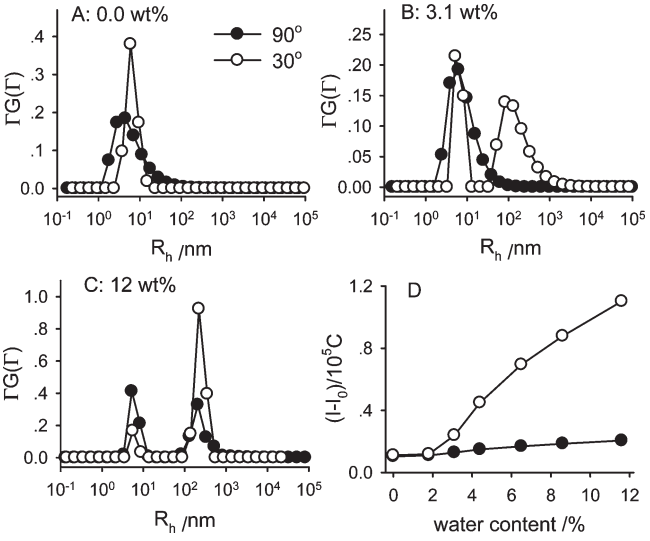


**Figure 1.** (A−C) CONTIN results of $PEGMA_{37}$-*b*-$MBPS_{141}$ at different water contents. (D) Changes in the excess scattered intensity. The initial concentration was 1.0 mg/mL.

## Results and Discussion

**Behavior of $PEGMA_{37}$-*b*-$MBPS_{141}$ in THF/$H_2O$: Thermodynamic Study.** THF is a good solvent for both PEGMA and PMBPS. The addition of water, a selective solvent for PPEGMA, would induce the aggregation of $PEGMA_{37}$-*b*-$MBPS_{141}$ when its content reached a certain ratio. As shown in Figure 1A, $PEGMA_{37}$-*b*-$MBPS_{141}$ stayed as single polymer chains in THF at 1.0 mg/mL. Its $R_{h,app}$ was about 7 nm. After adding 3.1 wt % water, an aggregate was observed at 30° (Figure 1B). The size and area ratio of the aggregate increased with increasing water content. At 12 wt % water, the aggregate with $R_{h,app}$ of 148 nm coexisted with the single polymer chains (Figure 1C). Further adding water led to a heavy turbidity, which deteriorates the quality of LLS data. Figure 1D shows that the excess scattered intensity increased almost linearly with the water content and displayed notable angular dependence after the appearance of aggregates at 3.1 wt % water.

The conformation of the aggregates could be inferred from the $R_{g,app}/R_{h,app}$ ratio.[45,46] Using the method proposed by Sato and co-workers,[47,48] we calculated the static structure factors ($S(q)$) of the slow mode by combining the data from SLS and DLS. The $R_{g,app}$ of the aggregate was then determined to be 102 nm from the $S(q)$ at 12 wt % water. So the $R_{g,app}/R_{h,app}$ ratios of the aggregates was calculated to be 0.69, close to the value (0.775) of solid sphere.[46] The presence of vesicle and disklike morphologies were ruled out because of their $R_{g,app}/R_{h,app}$ values should be close to 1.0 and larger than 1.5, respectively.[46,49,50] On the other hand, the contour length of $PEGMA_{37}$-*b*-$MBPS_{141}$ was calculated to be about 24 nm, far less than the $R_{h,app}$ of the aggregate (148 nm). Therefore, the aggregate formed by $PEGMA_{37}$-*b*-$MBPS_{141}$ was large compound micelles (LCM) instead of the primary micelles with PMBPS being the core and PEGMA being the corona.

Figure 2 shows the TEM images made from the above LLS solution at 12 wt % water content. Two types of spherical structures were observed. The large spherical structure with diameter more than 100 nm was attributed to the aggregates formed by $PEGMA_{37}$-*b*-$MBPS_{141}$. Since uranyl acetate

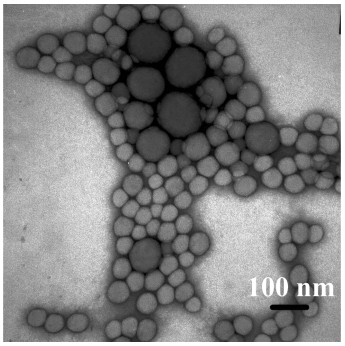


**Figure 2.** TEM images of $PEGMA_{37}$-*b*-$MBPS_{141}$ in THF with 12 wt % water.

mainly stained the PEGMA block, the dark hue of the large spheres confirmed the formation of large compound micelles.[5,44,51,52] The small spherical structure with diameter around 50 nm was attributed to primary micelles with PMBPS being the core and PEGMA being the corona. They were formed by the single polymer chains (Figure 1C) when pouring the solution to a large amount of water to prepare the sample for TEM.[44]

**Further Aggregation of LCMs to Cylinder: Kinetic Study.** The formation of the LCMs by $PEGMA_{37}$-*b*-$MBPS_{141}$ was observed right after adding water, and no other morphology was observed during the process of adding water to 12 wt % at ~2 wt % water per 1 h (Figure 1). The LCMs formed at the ending stage were stable; no morphology transition occurred in more than 24 h at room temperature. In the next experiment, we added 12 wt % water in one batch and monitored the system for more than 10 h. As shown in Figure 3, the bimodal distribution (Figure 3A) was maintained, but the size and area ratio of LCM increased with time and so did the excess scattered intensity (Figure 3B). After about 11 h, another aggregate with size in the order of micrometer was observed at 30°. Even though it was not distinguished at 90°, the broadening of the large fragment indicated the existence of the aggregate in the size of micrometer (Figure 3C). Since the excess scattered intensity was roughly proportional to the sixth power of size, the intensity-averaged size distribution in Figure 3C suggested that the number of the aggregate in micrometer was extremely small. Figure 3D shows the TEM image after 11 h. No micrometer scale structure but occasionally the fusion of few LCMs was visualized. Compared with Figure 2, the amount of LCMs increased.

It has been reported that the movement of single chains is easier with less selective solvent added.[53] In our next experiment, we added less amount (6.6 wt %) of water in $PEGMA_{37}$-*b*-$MBPS_{141}$ in one batch and monitored the kinetics. In this case, the micrometer aggregate became much clearer. As shown in Figure 4A, LCMs with $R_{h,app}$ peaked at 132 nm coexisted with the single chains once the experiment started. After an additional 2 h, the area ratio of the LCMs increased and the distribution narrowed (Figure 4B). At 5.5 h, the micrometer-scale aggregate was again observed at 30°, which was similar to that with 12 wt % water after 10 h (Figure 3C). The distribution at 90° was also broadened (Figure 4C). After 10 h, the large aggregate was observed at all the scattering angles, and its size and area ratio increased significantly. At this stage, the three components—single polymer chains, LCMs, and the newly formed aggregate—coexisted in the system (Figure 4D).

Figure 5A compares the correlation functions at 0.5 and 5.5 h at 30°. It clearly indicated the increase in the relaxation modes. However, the presence and the growth of the large

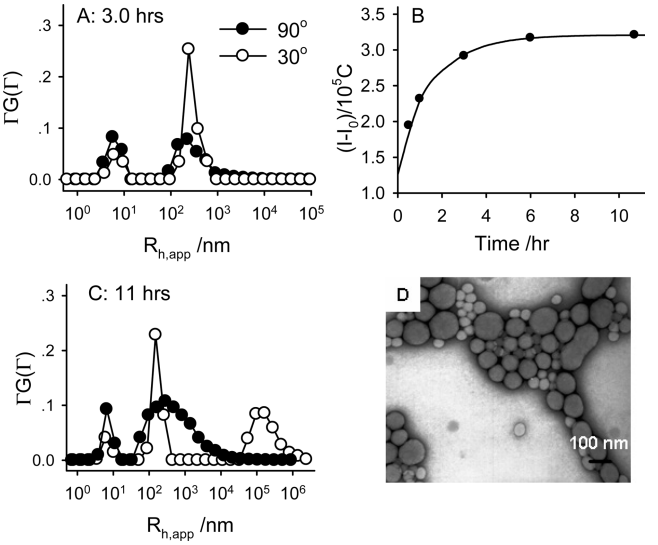


**Figure 3.** Aggregation of $PEGMA_{37}$-*b*-$MBPS_{141}$ in THF with 12 wt % water: (A) size distributions after 3.0 h; (B) time dependence of the excess scattered intensity at zero angle, the line is the fitting curve; (C) size distributions after 11 h; (D) TEM image after 11 h. The initial concentration was 1.0 mg/mL.

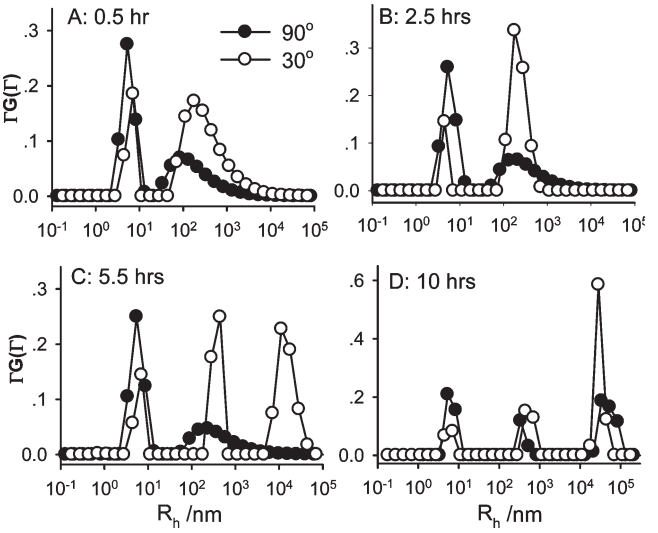


**Figure 4.** CONTIN results of $PEGMA_{37}$-*b*-$MBPS_{141}$ in THF with 6.6 wt % water contents after (A) 0.5, (B) 2.5, (C) 5.5, and (D) 10 h. The initial concentration was 1.0 mg/mL.

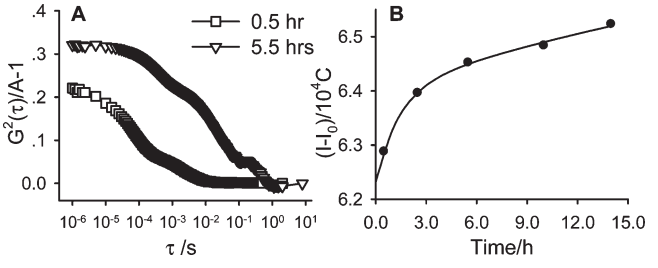


**Figure 5.** (A) Correlation functions at 0.5 and 5.5 h at 30°. (B) Time dependence of the excess scattered intensity of $PEGMA_{37}$-*b*-$MBPS_{141}$ in THF with 6.6 wt % water contents at zero angle; the line is the fitting curve. The initial concentration was 1.0 mg/mL.

aggregate exhibited a weak effect on the excess scattered intensity. As shown in Figure 5B, the sharp increase in the excess scattered intensity was observed before 5.5 h, during

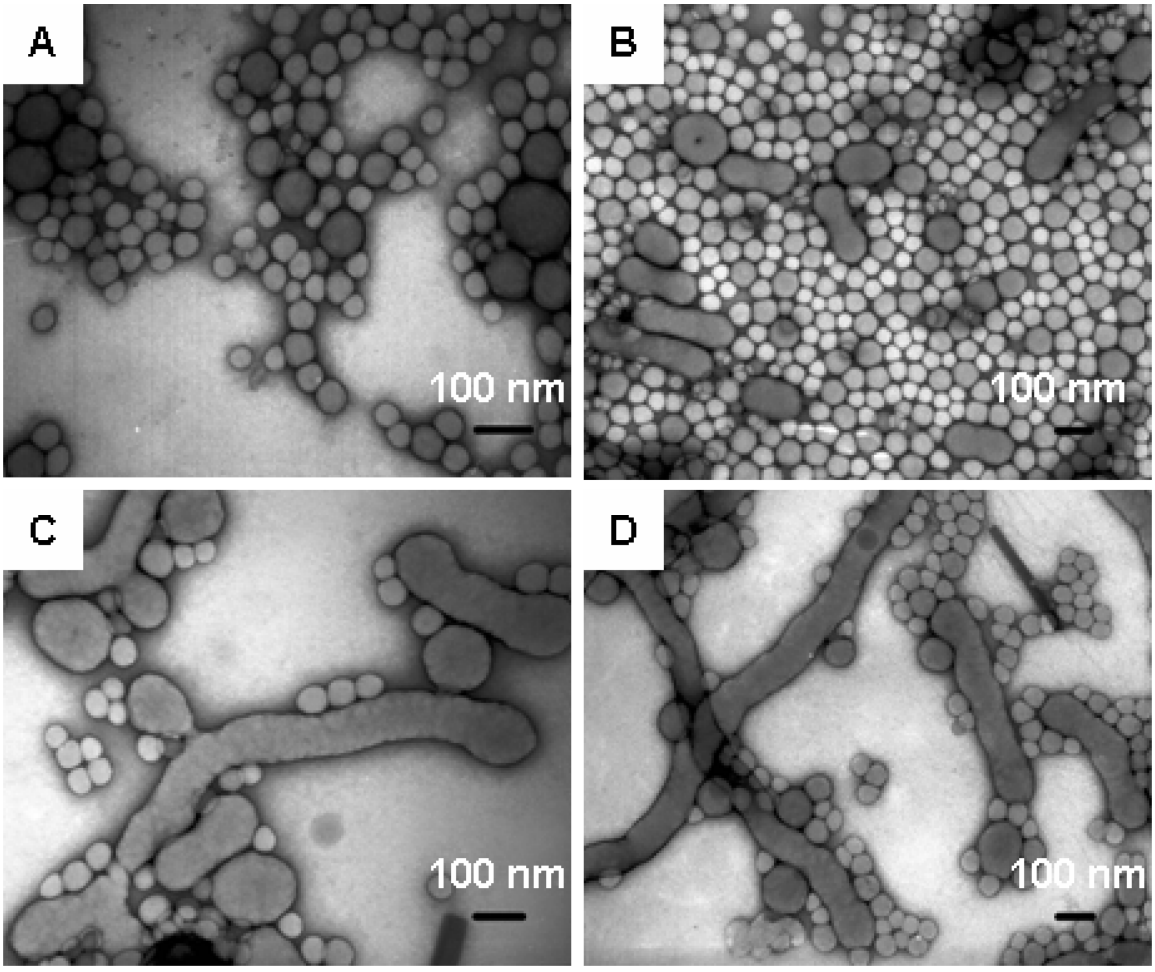


**Figure 6.** TEM results of $PEGMA_{37}$-*b*-$MBPS_{141}$ in THF with 6.6 wt % water at different aging times: (A) 2.5, (B) 5.5, and (C, D) 10 h. The initial concentration was 1.0 mg/mL.

which period the LCMs was formed and became matured. After the appearance of the micrometer size aggregate, the excess scattered intensity was kept almost constant, indicating that the growth in the large aggregate was at the cost of the LCMs instead of the single polymer chains.

The size of micrometer-scale aggregates surpasses the limit of our instrument. It was not valid to calculate the $R_{g,app}$ and the $R_{g,app}/R_{h,app}$ ratio of the aggregate by using Sato's approach.[47,48] Therefore, we conducted the TEM experiment. As shown in Figure 6A, after adding 6.6 wt % water for 2.5 h, only primary micelles and LCMs were observed, similar to those in Figure 2, which was also in agreement with the LLS data (Figure 4B). The connection and fusion of the spherical LCMs occurred at 5.5 h (Figure 6B). After 10 h, LCRs with length more than micrometer was observed in the system (Figure 6C,D). The large diameter and the dark hue indicated that the LCRs were formed by LCMs. Figure 6C also shows some branched sections on the LCRs. The coexistence of LCRs, LCMs, and primary micelles (formed by single polymer chains during quenching) after 10 h evidenced by TEM were consistent with the findings by LLS.

Besides water content, initial polymer concentration was another key parameter affecting the kinetics of the transition from LCMs to LCRs. Figure 7 shows the results of $PEGMA_{37}$-*b*-$MBPS_{141}$ at 0.1 mg/mL, a concentration diluted by a factor of 10. All other conditions are the same as those in Figure 4. As shown in Figure 7, the micrometer-scale aggregates were observed by DLS at 30° after 19 h (Figure 7A), about 3 times longer than that at 1.0 mg/mL. Its amount was also significantly reduced. The TEM image (Figure 7B) shows mainly primary micelles, LCMs, and a few occasionally fused LCMs.

**LCM-to-LCR Transition: Driving Forces.** Clearly, the formation of LCRs underwent two stages: aggregation of single polymer chains to form LCMs, followed by the fusion of LCMs to LCRs. The kinetics of the later stage was much slower than that of the former one. Since the excess scattered intensity is directly related with the morphological transition, we can evaluate the characteristic relaxation time, $\tau_1$ and $\tau_2$, by fitting the intensity curves (Figures 3B and 5B) with a double-exponential equation:

$$I = I_0 + A(1 - e^{-t/\tau_1}) + B(1 - e^{-t/\tau_2}) \quad (1)$$

where $t$ is time and $A$ and $B$ are adjustable parameters. The fitting in Figure 3B (12 wt % water) yielded $\tau_1 = 0.6$ min and $\tau_2 = 1.6$ h, indicating that the LCM-to-LCR transition was more than 150 times slower than the formation of LCM from single polymer chains. When the water content was reduced to 6.6 wt % (Figure 5B), the fitting curve gave $\tau_1 = 1.4$ h and $\tau_2 = 37$ h. The increase in $\tau_1$ by a factor of more than 100 suggested that the formation of LCM was highly dependent on water content. It was reasonable since the driving force for micelle was due to the selectivity of solvent. $\tau_2$ also increased with decreasing water content, but only by a factor of 23. Since LCR was formed via the fusion of LCM, the increased $\tau_2$, and the observance of large amount of LCR at earlier time (5.5 h at 6.6 wt % water, but 11 h at 12 wt %

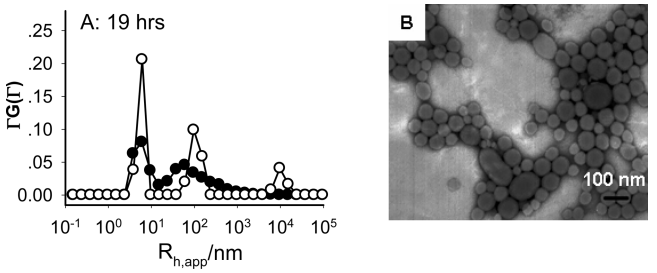


**Figure 7.** Aggregation of $PEGMA_{37}$-*b*-$MBPS_{141}$ in THF with 6.2 wt % water after 19 h: (A) size distributions; (B) TEM image. The initial concentration was 0.1 mg/mL.

water) suggested that LCR had a tendency to growth longer in length and greater in number at lower water content. The TEM images (Figures 6 and 3D) demonstrated this point.

It was commonly believed that the driving force for the sphere-to-rod transition was derived mainly from the elastic free energy of the core.[40] In our case, the LCMs did not have well-defined interface between the core and the corona. Therefore, the theory based on primary micelles may not be applied here. Since the LCM-to-LCR transition was prone to occur when adding water in one batch, it was controlled mainly by kinetics. The most possible explanation was that the freshly formed LCMs generated some defects on its surface. The defects could be a domain rich of PEGMA and water, or a small zone rich of PMBPS blocks, and they served as stick points to connect LCMs together. The initial aggregation of LCMs was not necessarily in rod morphology. However, fusion into rod decreased the surface tension or free energy. The TEM image in Figure 6C indicated the existence of the stick points connecting LCM and LCR together. Adding water dropwise and aging enough time to reach equilibrium "cured" most of the defects on LCM surface, preventing the occurrence of LCM-to-LCR transition. The formation of large amount of LCR at lower water content also supported this point.

Another new feature about $PEGMA_{37}$-*b*-$MBPS_{141}$ was that the single polymer chains existed throughout the LCM-to-LCR transition. Since the scattered intensity was roughly proportional to the sixth power of particle size, the amount of single polymer chains was pretty high even under the conditions where the micrometer-scale aggregate was fully developed, e.g., in the case of Figure 4D. The existence of the single polymer chains led to the attraction of the LCMs via the depletion effect.[54−63] Recently, Lodge and co-workers[57] demonstrated that the depletion interaction caused by homopolymer was able to effectively tune the morphology formed by block copolymers. According to Asakura and Oosawa,[54] the free energy gain, $\Delta F$, via depletion could be estimated by

$$\Delta F = \sim\left(1+\frac{3D}{2d}\right)\phi k_B T \qquad (2)$$

$D$ and $d$ are the diameters of the large and the small particles, and $\phi$ is the volume fraction occupied by the small particles. We can roughly estimate the $\phi$ value from the overlap concentration and the critical micelle concentration (cmc). Assume that the polymer chains are in random coil conformation, and $R_g = 1.5R_h = 10$ nm. The overlap concentration, $C^*$, was calculated according to

$$C^* = \frac{M_w}{\frac{4}{3}\pi R_g^3 N_A} \qquad (3)$$

with $N_A$ being Avogadro's number. The $C^*$ of $PEGMA_{37}$-*b*-$MBPS_{141}$ in THF was 31 mg/mL. The cmc of $PEGMA_{37}$-*b*-$MBPS_{141}$ in THF after adding 6.6 wt % water was determined by the dilution method (see Supporting Information). The obtained cmc value was 0.08 mg/mL, corresponding to the volume fraction of 0.08/31 = 0.0026. Taking the diameter of LCMs as 500 nm, the calculated energy gain by depletion attraction was about $0.1k_BT$. Even though the calculated value was much lower than $k_BT$, it could still make positive contribution to the LCM-to-LCR transition and could be used to qualitatively explain the observed phenomena. In the case of adding 12 wt % water, the cmc was much smaller, leading to a negligible attraction between LCMs, and thus weakened the formation of LCR (Figure 3). When the concentration was diluted by a factor of 10, the depletion attraction was the same since its concentration was still above cmc, but the amount of LCMs was sharply reduced (Figure 7). During the sphere-to-rod transitions of regular micelles, the single polymer chains may also exist, but they are difficult to be detected because of the small size.

## Conclusions

Using the LCMs formed by rod−coil diblock copolymer, $PEGMA_{37}$-*b*-$MBPS_{141}$, as an example, we monitored the kinetics of sphere-to-rod transition by time-resolved laser light scattering. Our study revealed that both the instability (or defect) of the sphere and the depletion force generated by the free polymer chains made positive contributions to the sphere-to-rod transition. This rule may also be applied to the transitions of even more complicated morphologies. Actually, the depletion effect, originated from entropy, has been proven to account for the formation of many advanced structures in cellular environment. Our study, based on a simple mode, not only helps in the preparation of desirable morphology by using synthetic polymers but also gains insight into the mechanism of the complicated process in cellular activity.

**Acknowledgment.** This work is financially supported by the National Natural Science Foundation of China (Grants 20774004 and 20674001) and the National Distinguished Young Scholar Fund (Grant 20325415).

**Supporting Information Available:** The cmc of $PEGMA_{37}$-*b*-$MBPS_{141}$ in THF with 6.6 wt % water. This material is available free of charge via the Internet at http://pubs.acs.org.

## References and Notes

(1) Lehn, J. M. *Supramolecular Chemistry*; VCH: Weiheim, 1995.
(2) Hadjichristidis, N.; Pispas, S.; Floudas, G. *Block Copolymers: Synthetic Strategies, Physical Properties, and Applications*; John Wiley & Sons: Hoboken, NJ, 2003.
(3) Halperin, A. *Macromolecules* **1987**, *20*, 2943–2946.
(4) Stupp, S. I.; Son, S.; Lin, H. C.; Li, L. S. *Science* **1993**, *259*, 59–63.
(5) Zhang, L.; Eisenberg, A. *Science* **1995**, *268*, 1728–1731.
(6) Zhang, L.; Eisenberg, A. *J. Am. Chem. Soc.* **1996**, *118*, 3168–3181.
(7) Discher, B. M.; Won, Y.-Y.; Ege, D. S.; Lee, J. C.-M.; Bates, F. S.; Discher, D. E.; Hammer, D. A. *Science* **1999**, *284*, 1143–1146.
(8) Lee, M.; Cho, B. K.; Zin, W. C. *Chem. Rev.* **2001**, *101*, 3869–3892.
(9) Vriezema, D. M.; ComellasAragones, M.; Elemans, J. A. A. W.; Cornelissen, J. J. L. M.; Rowan, A. E.; Nolte, R. J. M. *Chem. Rev.* **2005**, *105*, 1445–1489.
(10) Jain, S.; Bates, F. S. *Science* **2003**, *300*, 460–464.
(11) Whitesides, G. M.; Simanek, E. E.; Mathias, J. P.; Seto, C. T.; Chin, D. N.; Mammen, M.; Gordon, D. M. *Acc. Chem. Res.* **1995**, *28*, 37–44.
(12) Cameron, N. S.; Corbierre, M. K.; Eisenberg, A. *Can. J. Chem.* **1999**, *77*, 1311–1326.
(13) Iyama, K.; Nose, T. *Macromolecules* **1998**, *31*, 7356–7364.
(14) Chen, L.; Shen, H.; Eisenberg, A. *J. Phys. Chem. B* **1999**, *103*, 9488–9497.

(15) Yu, K.; Zhang, L.; Eisenberg *Langmuir* **1996**, *12*, 5980–5984.
(16) Jenekhe, S. A.; Chen, X. L. *Science* **1998**, *279*, 1903–1907.
(17) Tu, Y.; Wan, X.; Zhang, D.; Zhou, Q.; Wu, C. *J. Am. Chem. Soc.* **2000**, *122*, 10201–10205.
(18) Kim, B. S.; Hong, D. J.; Bae, J.; Lee, M. *J. Am. Chem. Soc.* **2005**, *127*, 16333–16337.
(19) Tung, Y. C.; Wu, W. C.; Chen, W. C. *Macromol. Rapid Commun.* **2006**, *27*, 1838–1844.
(20) Lin, S. L.; Numasawa, N.; Nose, T.; Lin, J. P. *Macromolecules* **2007**, *40*, 1684–1692.
(21) Lee, H.; Jakubowski, W.; Matyjaszewski, K.; Yu, S.; Sheiko, S. S. *Macromolecules* **2006**, *39*, 4983–4989.
(22) Cheng, Z. P.; Zhu, X. L.; Kang, E. T.; Neoh, K. G. *Macromolecules* **2005**, *38*, 7187–7192.
(23) Ishizone, T.; Han, S.; Hagiwara, M.; Yokoyama, H. *Macromolecules* **2006**, *39*, 962–970.
(24) Discher, D. E.; Eisenberg, A. *Science* **2002**, *297*, 967–973.
(25) Choucair, A. A.; Kycia, A. H.; Eisenberg, A. *Langmuir* **2003**, *19*, 1001–1008.
(26) Porte, G.; Gomati, R.; Haitamy, O. E.; Appell, J.; Marignan, J. *J. Phys. Chem.* **1986**, *90*, 5746–5751.
(27) Yan, D.; Zhou, Y.; Hou, J. *Science* **2004**, *303*, 65–67.
(28) Wang, C. Y.; Lodge, T. P. *Macromolecules* **2002**, *35*, 6997–7006.
(29) Zhou, Z.; Chu, B. *Macromolecules* **1988**, *21*, 2548–2554.
(30) Schillen, K.; Brown, W.; Johnsen, R. M. *Macromolecules* **1994**, *27*, 4825–4832.
(31) Mortensen, K.; Pedersen, J. S. *Macromolecules* **1993**, *26*, 805–812.
(32) Burke, S.; Eisenberg, A. *Langmuir* **2001**, *21*, 6705–6714.
(33) Ma, Q.; Remsen, E. E., Jr.; Clark, C. G.; Kowalewski, T.; Wooley, K. L. *Proc. Natl. Acad. Sci. U.S.A.* **2002**, *99*, 5058–5063.
(34) Denkova, A. G.; Mendes, E.; Coppens, M.-O. *J. Phys. Chem. B* **2009**, *113*, 989–996.
(35) Shen, L.; Wang, H.; Guerin, G.; Wu, C.; Manners, I.; Winnik, M. A. *Macromolecules* **2008**, *41*, 4380–4389.
(36) Wang, X.; Guerin, G.; Wang, H.; Wang, Y.; Manners, I.; Winnik, M. A. *Science* **2007**, *317*, 644–647.
(37) Korczagin, I.; Hempenius, M. A.; Fokkink, R. G.; Cohen Stuart, M. A.; Al-Hussein, M.; Bomans, P. H. H.; Frederik, P. M.; Vancso, G. J. *Macromolecules* **2006**, *39*, 2306–2315.
(38) LaRue, I.; Adam, M.; Pitsikalis, M.; Hadjichristidis, N.; Rubinstein, M.; Sheiko, S. S. *Macromolecules* **2006**, *39*, 309–314.
(39) Lodge, T. P.; Bang, J.; Li, Z.; Hillmyer, M. A.; Talmon, Y. *Faraday Discuss.* **2005**, *128*, 1–12.
(40) Zhulina, E. B.; Adam, M.; LaRue, I.; Sheiko, S. S.; Rubinstein, M. *Macromolecules* **2005**, *38*, 5330–5351.
(41) Kaewsaiha, P.; Matsumoto, K.; Matsuoka, H. *Langmuir* **2007**, *23*, 9162–9169.
(42) Lehner, D.; Helmut, L.; Glatter, O. *Langmuir* **2000**, *16*, 1689–1695.
(43) Ji, W.; Yan, J.; Chen, E.; Li, Z.; Liang, D. *Macromolecules* **2008**, *41*, 4914–4919.
(44) Cao, H.; Lin, W.; Liu, A.; Zhang, J.; Wan, X.; Zhou, Q. *Macromol. Rapid Commun.* **2007**, *28*, 1883–1888.
(45) Burchard, W. *Adv. Polym. Sci.* **1983**, *48*, 1–124.
(46) Huglin, M. B., Ed. *Light Scattering from Polymer Solution*; Academic Press: London, 1972; p 132.
(47) Kanao, M.; Matsuda, Y.; Sato, T. *Macromolecules* **2003**, *36*, 2093–2102.
(48) Aono, H.; Tatsumi, D.; Matsumoto, T. *Biomacromolecules* **2006**, *7*, 1311–1317.
(49) Wu, J.; Pearce, E. M.; Kwei, T. K.; Lefebvre, A. A.; Balsara, N. P. *Macromolecules* **2002**, *35*, 1791–1796.
(50) Zhou, S.; Burger, C.; Chu, B.; Sawamura, M.; Nagahama, N.; Toganoh, M.; Hackler, U. E.; Isobe, H.; Nakamura, E. *Science* **2001**, *291*, 1944–1947.
(51) Monneron, A.; Bernhard, W. *J. Ultrastruct. Res.* **1969**, *27*, 266–288.
(52) Burkoth, T. S.; Benzinger, T. L. S.; Jones, D. N. M.; Hallenga, K.; Meredith, S. C.; Lynn, D. G. *J. Am. Chem. Soc.* **1998**, *120*, 7655–7656.
(53) Zhang, L. F.; Eisenberg, A. *Macromolecules* **1999**, *32*, 2239–2249.
(54) Asakura, S.; Oosawa, F. *J. Polym. Sci.* **1958**, *33*, 183–192.
(55) Pace, C. N.; Shirley, B. A.; McNutt, M.; Gajiwala, K. *FASEB J.* **1996**, *10*, 75–83.
(56) Marenduzzo, D.; Finan, K.; Cook, P. R. *J. Cell Biol.* **2006**, *175*, 681–686.
(57) Abbas, S.; Lodge, T. P. *Phys. Rev. Lett.* **2007**, *99*, 137802–137805.
(58) Adams, M.; Dogic, Z.; Keller, S. L.; Fraden, S. *Nature* **1998**, *393*, 349–352.
(59) Yang, S.; Yan, D.; Tan, H.; Shi, A. C. *Phys. Rev. E* **2006**, *74*, 041808(10).
(60) Yang, S.; Tan, H.; Yan, D.; Nies, E.; Shi, A. C. *Phys. Rev. E* **2007**, *75*, 061803(7).
(61) Urakami, N.; Imai, M. *J. Chem. Phys.* **2003**, *119*, 2463–2470.
(62) Zhou, D.; Zhang, J.; Li, L.; Xue, G. *J. Am. Chem. Soc.* **2003**, *125*, 11774–11775.
(63) Li, L.; Zhou, D.; Zhang, J.; Xue, G. *J. Phys. Chem. B* **2004**, *108*, 5153–5156.